J. Non-Newtonian Fluid Mech. 132 (2005) 53–60

Journal of Non-Newtonian Fluid Mechanics

www.elsevier.com/locate/jnnfm

Transient solutions of the dynamics of film casting process using a 2-D viscoelastic model

Ju Min Kim, Joo Sung Lee, Dong Myeong Shin, Hyun Wook Jung*, Jae Chun Hyun

Department of Chemical and Biological Engineering, Applied Rheology Center, Korea University, Seoul 136-701, Korea

Received 6 November 2004; received in revised form 16 June 2005; accepted 1 October 2005

Abstract

The nonlinear transient dynamics and stability of a two-dimensional (2-D) model of the isothermal film casting process have been investigated using newly devised simulation techniques employing finite element methods (FEM), which can incorporate the viscoelastic nature of polymer melts as well as the Newtonian features of other fluids. To effectively solve the time-dependent free surface problem of this system, the Arbitrary Lagrangian Eulerian (ALE) algorithm together with a spine method well-suited for free surface tracking was incorporated. Adopting robust numerical stabilization techniques for the hyperbolic system of extensional deformation processes in this study, the transient dynamic behavior of viscoelastic fluids in the 2-D film casting process are presented for the first time in the literature. It is also demonstrated that simulation models in the present study can successfully describe the basic flow behavior of the system including the three instability modes therein, i.e., draw resonance, neck-in, and development of edge beads.

Keywords: Film casting; FEM; ALE; Spine method; Draw resonance; Edge beads; Neck-in; Stability; Transient behavior; Viscoelastic fluids

1. Introduction

The film casting process is a high-speed process for making highly oriented film in which a molten film is extruded through a slit die and rapidly stretched in the machine direction by rotation of the chill roll (Fig. 1). However, many kinds of process disturbances inevitably affect the productivity and uniformity of the film. The defects caused by these disturbances are typically classified into three different modes. First, draw resonance which is characterized by periodic oscillations of state variables such as film thickness, film width, and tension, arises as the drawdown ratio is increased beyond its critical value. The same phenomenon also occurs in other extensional deformation processes, e.g., fiber spinning and film blowing. Because of its academic and industrial importance as a research topic or a productivity issue, draw resonance has attracted many researchers to carry out important stability studies of the processes during the past four decades [1–8]. Second, there is also the problem of the reduction of the film width, called neck-in: the width of polymeric film extruded from a flat die shrinks along the machine direction due to the strong extensional deformation effected by the pull of the chill roll. To prevent this neck-in, it is common to keep the distance between the die and chill roll as short as possible. Third, edge beads or 'dog-bone' phenomenon also arise in the film casting process: thicker beads at the film edges than those at the center are formed, resulting in the unevenness of the final film product.

The above three instability modes in film casting have been studied by many researchers, most notably by Agassant' and Co' groups, using (a) 1-D models to illustrate draw resonance phenomenon with the simplifying assumption of the constant film width [4,9];(b) other improved 1-D models that can predict both draw resonance phenomenon and the neck-in [6,10–13], and (c) 2-D or 3-D models which can describe the edge beads as well as the above two instabilities [5,14–16].

By adopting a membrane model, Agassant's group produced for the first time the transient behavior of the Newtonian case using a tracking strategy for the deformed rectangular mesh and a capturing strategy with a continuous finite element method for film velocity and discontinuous finite element for film thickness. Co's group studied the draw resonance instability of various viscoelastic fluids using linear stability analysis on time and spatial variations of state variables [4,9]. However, the transient

* Corresponding author. Tel.: +82 2 3290 3306; fax: +82 2 926 6102.
E-mail address: hwjung@grtrkr.korea.ac.kr (H.W. Jung).

0377-0257/$ – see front matter
doi:10.1016/j.jnnfm.2005.10.002

Nomenclature

A_r	aspect ratio ($\equiv L/w_0$)
B_r	bead ratio ($\equiv e_{edge}/e_{center}$)
$\boldsymbol{D}$	rate of deformation tensor
De	Deborah number ($\equiv \lambda v_0/L$)
D_r	draw ratio ($\equiv v_L/v_0$)
e	film thickness
$\mathbf{J}$	Jacobian matrix
L	distance from die exit to chill roll
$\boldsymbol{n}$	normal vector
P	isotropic pressure
$\boldsymbol{q}$	state variables
$\mathbf{R}$	residual set of nonlinear governing equations
t	elapsed time
$\boldsymbol{v}$	velocity vector with components v_x and v_y in x- and y-directions, respectively
$\boldsymbol{v}^m$	mesh velocity
w	film width

Greek letter

δ	step disturbance at take-up velocity initiating dynamic response of the system
ϕ	linear shape function
η	zero shear viscosity
λ	fluid relaxation time
$\boldsymbol{\sigma}$	total stress tensor
$\boldsymbol{\tau}$	extra stress tensor
ψ	bilinear shape function

Subscript

0	die exit
L	chill roll position
x	flow direction (machine direction)
y	transverse direction
z	normal direction to the film surface

solution for viscoelastic fluids in 2-D film casting has not been reported yet.

Several noteworthy research results have been reported recently: Smith and Stolle [15] successfully solved the non-isothermal 2-D governing equations with the finite element method (FEM), concluding that the neck-in phenomenon can be suppressed by the self-weight of the film, nonisothermal conditions, or nonuniform boundary conditions at the die exit. Satoh et al. [16] also solved 2-D equations using Galerkin FEM with streamline elements for continuity and momentum equations. Sakaki et al. [14] first reported a 3-D model of the Newtonian film casting. Despite significant progress made by these efforts, there still remains the need for transient solutions of viscoelastic film casting and the fundamental understanding of the physics behind the instabilities.

In this study, the nonlinear dynamics and stability of the 2-D film casting process have been scrutinized using up-to-date numerical FEM techniques for steady and transient computations. For the transient simulations of 2-D Newtonian and viscoelastic film castings with free surfaces, guaranteeing the exact portrayal of all interesting phenomena such as draw resonance, neck-in, and edge beads, the Arbitrary Lagrangian Eulerian (ALE) algorithm with spine method was employed [17–25]. These robust numerical schemes provide all the essential information enabling steering the process into the stable region and also reveal strategies to enlarge the stability window of the process.

2. Mathematical modeling

For Newtonian and Upper-Convected Maxwell (UCM) fluids, the governing equations for the 2-D film casting are shown below based on the model by Silagy et al. [5]. Fig. 1 depicts schematic geometry and boundaries for this system.

$$\text{Equation of continuity}: \quad \frac{\partial e}{\partial t} + \nabla \cdot e\boldsymbol{v} = 0. \tag{1}$$

$$\text{Equation of motion}: \quad \nabla \cdot e\boldsymbol{\sigma} = 0. \tag{2}$$

Constitutive equations

$$\text{Newtonian fluids}: \quad \boldsymbol{\tau} = 2\eta\boldsymbol{D}. \tag{3a}$$

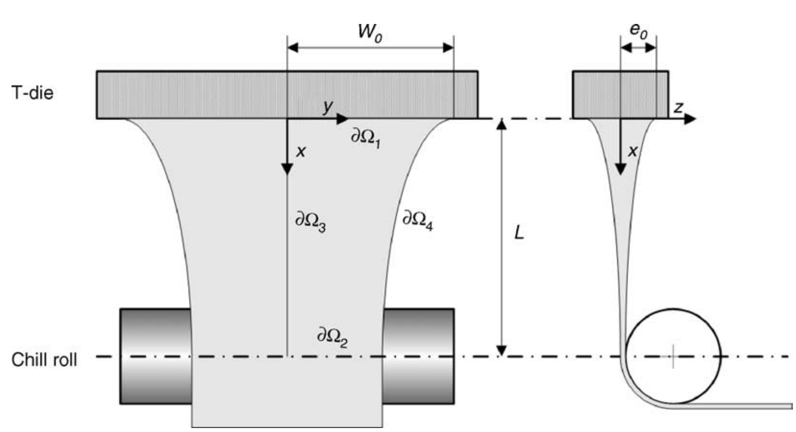

Fig. 1. Schematic diagram for the film casting process.

Upper-Convective Maxwell (UCM) fluids :

$$\boldsymbol{\tau}+\lambda\left[\frac{\partial\boldsymbol{\tau}}{\partial t}+\boldsymbol{v}\cdot\nabla\boldsymbol{\tau}-(\nabla\boldsymbol{v})^{T}\cdot\boldsymbol{\tau}-\boldsymbol{\tau}\cdot(\nabla\boldsymbol{v})\right]=2\eta\boldsymbol{D}. \tag{3b}$$

Boundary conditions

(i) Inlet : $v_x=v_0,\ \ v_y=0,\ \ e=e_0,\ \ w=w_0,\ \ \boldsymbol{\tau}=\boldsymbol{\tau}_0$ on $\partial\Omega_1$ at $t=0$. (4a)

$$v_x=v_0,\ \ v_y=0,\ \ e=e_0,\ \ w=w_0\quad \text{on}\quad \partial\Omega_1\quad \text{at}\ t>0. \tag{4b}$$

(ii) Outlet : $v_x=v_{\rm L},\ \ v_y=0$ on $\partial\Omega_2$ at $t=0$. (4c)

$$v_x=v_{\rm L}(1+\delta),\ \ v_y=0,\quad \text{on}\quad \partial\Omega_2\quad \text{at}\ t>0. \tag{4d}$$

(iii) Center : $\sigma_{xy}=0$ on $\partial\Omega_3$ at $t\geq 0$. (4e)

(iv) Edge : $\dfrac{\partial w}{\partial t}+v_x\dfrac{\partial w}{\partial x}=v_y,\quad \boldsymbol{\sigma}\cdot\boldsymbol{n}=0$ on $\partial\Omega_4$ at $t\geq 0$. (4f)

(The detailed notations are given in the Nomenclature.)

If the curvature of film is small, state variables do not depend on the film thickness direction, also total stress in this direction (σ_{zz}) should be zero, meaning the isotropic pressure is equal to the normal stress (τ_{zz}). It is noted that inlet stresses at the die exit for the steady calculations of viscoelastic film casting were taken from Newtonian values under the same operating conditions, not affecting the downstream solutions [10,16] and were considered as unknowns during transient simulations.

3. Numerical methods

Although there have been many valuable studies on the linear and nonlinear stability analyses of the film casting systems employing (a) constant film width 1-D models [4,9]; (b) varying film width 1-D models [10,11,13], and (c) 2-D models [5], there exist only a few reports on transient responses of 2-D film casting process: e.g., the results of Newtonian fluids by Silagy et al. [5]. In this study, we have devised new numerical schemes for the film casting of viscoelastic fluids to report steady state solutions first, and then transient solutions.

3.1. Scheme for steady-state solutions

The film casting flow is evaluated using the governing Eqs. (1)–(4) with the finite element method (FEM). The velocity, extra stress, film thickness, and film width were approximated using Lagrangian basis functions as shown in Eq. (5).

$$\boldsymbol{v}=\sum_i\psi_i\boldsymbol{v}_i,\quad \boldsymbol{\tau}=\sum_i\psi_i\boldsymbol{\tau}_i,\quad e=\sum_i\psi_i e_i,\quad w=\sum_i\phi_i w_i, \tag{5}$$

where ψ_i denotes a bilinear shape function and ϕ_i is a linear shape function. The computational domain Ω was discretized into quadrilateral finite elements $R_{\rm e}$ so that $\Omega=\cup R_{\rm e}$ and $\emptyset=\cap R_{\rm e}$.

The algebraic equations of the weighted residuals for UCM fluids are shown below.

$$\text{Equation of continuity}:\ \langle\boldsymbol{v}\cdot\nabla e+e\nabla\cdot\boldsymbol{v};\psi\rangle=0. \tag{6}$$

$$\text{Equation of motion}:\ \langle e\boldsymbol{\sigma};\nabla\psi\rangle=\langle\langle e\boldsymbol{\sigma}\cdot\boldsymbol{n};\psi\rangle\rangle. \tag{7}$$

Constitutive equation :

$$\left\langle\boldsymbol{\tau}+\lambda\left[\boldsymbol{v}\cdot\nabla\boldsymbol{\tau}-(\nabla\boldsymbol{v})^{\rm T}\cdot\boldsymbol{\tau}-\boldsymbol{\tau}\cdot(\nabla\boldsymbol{v})\right]-2\eta\boldsymbol{D};\psi\right\rangle=0. \tag{8}$$

$$\text{Kinematic equation}:\ \left\langle\left\langle v_x\frac{\partial w}{\partial x}-v_y;\phi\right\rangle\right\rangle=0. \tag{9}$$

Integration by parts and the divergence theorem are applied to equations of motion; ⟨A;B⟩ indicates $\int_{\rm e}AB{\rm d}\Omega_{\rm e}$ surface integral on the element; ≪A;B≫ denotes $\int_{\partial\Omega_{\rm e}}AB{\rm d}\partial\Omega_{\rm e}$ line integral on the boundaries of finite elements. Pressure terms were eliminated from the governing equations by the relationship $\sigma_{zz}=-P+\tau_{zz}=0$. The stress $\boldsymbol{\tau}$ includes three extensional stress components and one shear stress component in xy-domain. Other stress components are assumed to be zero.

Unlike Silagy et al. [5] who considered total stress formulation comprising only x and y, not z component, using the membrane approximation and thus eliminated the extra stress, τ_{zz}, the model in this study directly employed the original extra stresses in its entirety without any modification. It is thus noted that the stress formulation by Silagy et al. [5] is different from this study because their total stress equation cannot be derived from the constitutive equations of this study.

Since the convection terms in the continuity and kinematic equations could destabilize the overall system numerically, streamline upwinding/Petrov Galerkin (SU/PG) method [21,22] is employed to make the weighting function skewed toward the upstream direction at each computational node.

The above set of governing equations is solved by the Newton-Raphson method as expressed below in simple vector forms.

$$\boldsymbol{J}(\boldsymbol{q}^{\rm s})\Delta\boldsymbol{q}=-\boldsymbol{R}(\boldsymbol{q}^{\rm s}). \tag{10}$$

where **R** denotes the residual set of nonlinear governing equations, $\boldsymbol{q}(e,\boldsymbol{v},\boldsymbol{\tau},w)$ are state variables, $\boldsymbol{J}(\boldsymbol{q}^{\rm s})\equiv\partial\boldsymbol{R}(\boldsymbol{q}^{\rm s})/\partial\boldsymbol{q}$ is the Jacobian matrix, and the superscript s represents the previous step at each iteration. The unknowns including free surface profile are iteratively updated with the relationship $\boldsymbol{q}^{\rm s+1}=\boldsymbol{q}+\Delta\boldsymbol{q}$ until the convergence criterion, i.e., ${\rm MAX}((\Delta e/e_{\max}),(\Delta v_i/v_{i,\max}),(\Delta\tau_{ij}/\tau_{ij,\max}),(\Delta w/w_{\max}))<10^{-4}$ is satisfied, where superscript s+1 denotes the updated step. During the iterations, $\Delta\boldsymbol{q}$ is obtained using a direct frontal solver [23] with the prescribed boundary conditions (4). In this study, uniformly distributed rectangular meshes were used at the initial stage and locations of inner nodes were redistributed using the spine method [24]. The initial distance ratio of inner nodes from the center to the free surface nodes is prescribed as follows.

$$h_i=\beta_i w(y,t),\qquad \beta_i=\frac{h_{0i}}{w_0}. \tag{11}$$

where w_0 represents the distance between the center and the film edge (the free surface) and h_{0i} the distance of inner nodes from the center in the initial rectangular meshes. β_i is kept constant during the computations. One interesting point of this algorithm is that unlike Silagy et al. [5], the coupled equations comprising unknown state variables and the location of free surface are simultaneously solved at each iteration step.

3.2. Scheme for transient solutions

The time-dependent terms of governing equations embedded in Eqs. (1), (3b), and (4d) must be treated carefully in the transient simulation since the computational nodes are varied at every time step due to the temporal motion of free surfaces. We modified the material time derivative terms in the continuity and the constitutive equations using the ALE formulation [25], as shown below.

$$\frac{\mathrm{D}()}{\mathrm{D}t}=\frac{\partial()}{\partial t}+(\boldsymbol{v}-\boldsymbol{v}^{\mathrm{m}})\cdot\nabla(). \tag{12}$$

where $\boldsymbol{v}^{\mathrm{m}}$ denotes the mesh velocity which is equal to $\boldsymbol{v}$ at the free surface. Mesh nodes at the free surface move in the Lagrangian framework and the velocities of inner nodes are determined from those on the free surfaces by a spine method. The transient terms are evaluated using an unconditionally stable 2nd-order Gear method to avoid numerical instability. The error tolerance is prescribed such that the relative error of the new and previous steps is below 10^{-9} and the same criterion as in the Newton-Raphson algorithm for solving steady states (10^{-4}) is applied at each time step.

4. Results and discussion

4.1. Implementation of numerical algorithms

In the film casting system considered here, there are three most influential processing parameters affecting the dynamical behavior, i.e., draw ratio ($D_{\mathrm{r}} \equiv v_{\mathrm{L}}/v_0$), Deborah number ($De = \lambda v_0/L$), and aspect ratio ($A_{\mathrm{r}} \equiv L/w_0$) (see Fig. 1). The optimal mesh tessellation used here is 35×35, guaranteeing the acceptable accuracy for the steady and transient calculations. Fig. 2 depicts the final mesh structure and the steady profiles of the film thickness and film width of the viscoelastic fluid with $D_{\mathrm{r}} = 15$, $A_{\mathrm{r}} = 0.6$, and $De = 0.001$, clearly showing both neck-in and edge beads.

In the viscoelastic case, the results of the film thickness and film width profiles by this study are quite different from those by Silagy et al. [5], as shown in Fig. 3. This is because they used a different stress formulation than ours. It is believed that fully including τ_{zz} term into the model as an unknown in this study produces more reasonable results, as it should. It is also found in this study that viscoelasticity as measured by the Deborah number, De, appears to suppress the neck-in of the system.

In order to confirm the proposed transient numerical algorithm and computing codes, we first obtained the new steady solution using transient computations in a stable region and compared it with that by the steady algorithm. The numerical algorithms are found to be robust and reliable, proving that the converged transient solutions ultimately match their stationary ones, as they should, even with the large time step size employed (e.g., $\Delta t = 1.0$) in the stable regimes. This is in sharp contrast to previous results reported by other researchers [5] where the two did not match each other and small artificial thickness fluctuations at the free surface were noticed. In the unstable regimes it was found that smaller time steps than for stable regimes were required for numerical stability. The optimal time step size for unstable regimes, i.e., draw resonance, was found to be $\Delta t = 0.005$.

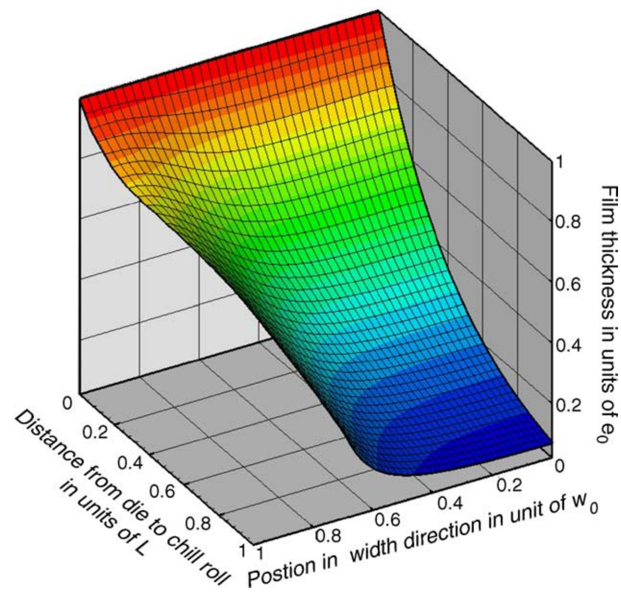

Fig. 2. Neck-in and edge bead phenomena for the viscoelastic fluid at $D_{\mathrm{r}} = 15$, $A_{\mathrm{r}} = 0.6$, $De = 0.01$.

4.2. Steady state analysis: neck-in and edge beads

The neck-in and edge beads phenomena inevitably encountered in the film casting process should be strictly controlled

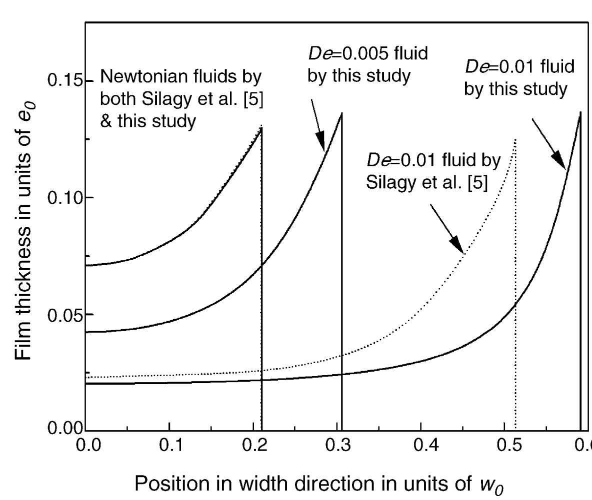

Fig. 3. Comparison of steady profiles by Silagy et al. [5] and this study: the film thickness at take-up for viscoelastic and Newtonian fluids ($D_{\mathrm{r}} = 50$ and $A_{\mathrm{r}} = 1.0$).

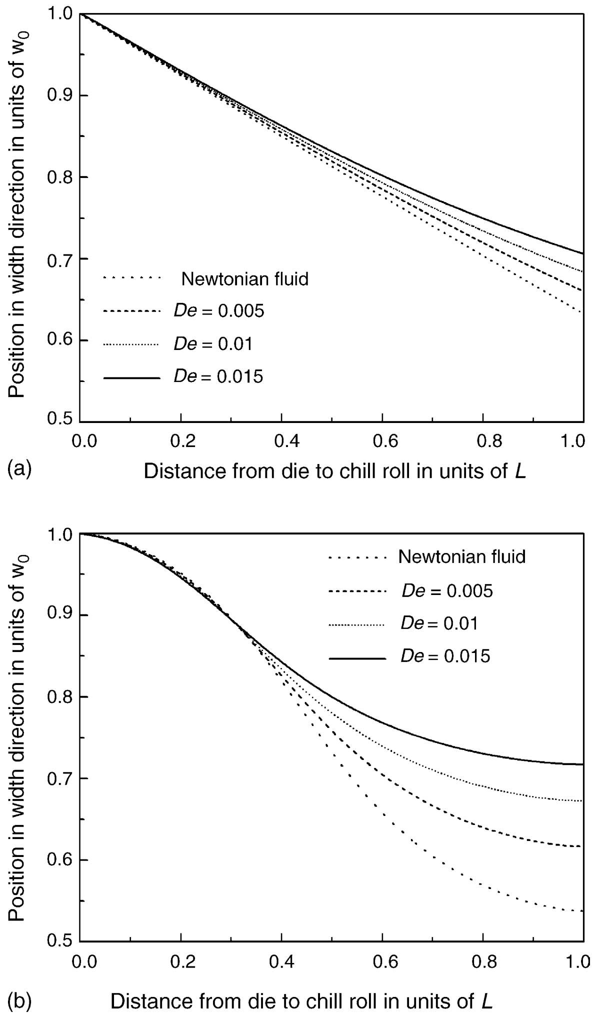

Fig. 4. Film width profiles by (a) 1-D model and (b) by 2-D model for viscoelastic and Newtonian fluids with $A_r = 0.6$ and $D_r = 20$.

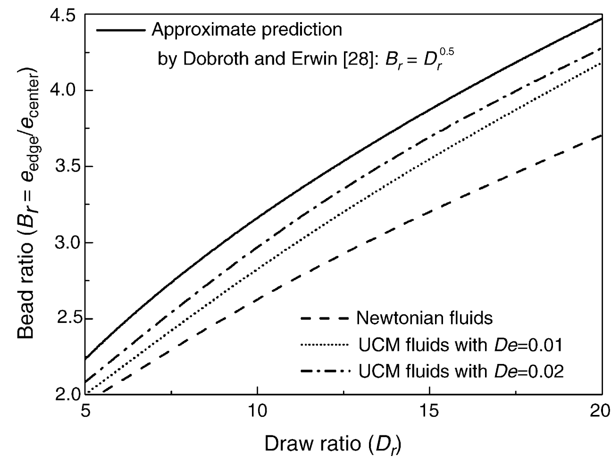

Fig. 5. Comparison of bead ratios results at $A_r = 0.6$ by the 2-D model of this study with the simple relationship by Dobroth and Erwin [28].

for process productivity and product quality. The film width profiles by the present 2-D model are compared with those by previous 1-D models [10,11,13] in Fig. 4. The 2-D model by this study predicts more reasonable neck-in behavior, depending on the viscoelasticity or the Deborah number (De), than 1-D model, although both models show the similar tendency of neck-in decreasing with the Deborah number (De).

The formation of edge beads is primarily due to the differences in stresses (or rate of deformation) between the edge and center regimes of the film, especially for the highly viscous materials. Dobroth and Erwin [28] suggested the approximate relationship for the bead ratio (B_r), defined as the ratio of the film thickness at the edge and at the center of the take-up position, by assuming the planar extensional flow in the center and the uniaxial extensional flow at the edge. This simple equation of the square root of draw ratio overestimates the bead ratio, compared to that of this study as shown in Fig. 5 because two basic extensional flows can not be completely separated at each position in the film in real processes. Interestingly, it has been also found in Fig. 5 that bead ratio data of this study approach the simple equation as the fluid viscoelasticity rises. This is because the increasing De makes the smaller neck-in in the film width allowing more planar extensional flow at the center, thus the results coming closer to the Dobroth and Erwin's estimates.

Fig. 6 shows the effects of various process conditions such as draw ratio (D_r), aspect ratio (A_r), and Deborah number (De) on the film thickness and film width profiles at the take-up position. The neck-in is shown to decrease with the decreasing D_r and A_r, and the increasing De, whereas the bead ratio is reduced with the decreasing D_r and De, and the increasing A_r under the chosen conditions.

4.3. Transient analysis: draw resonance

The nonlinear transient analysis is indispensable for analyzing the physics and mechanism of flow instability such as draw resonance, a supercritical Hopf bifurcation. Transient responses of 1-D film casting system have been reported before [9,10,13], but reports on 2-D transient responses have been done only for Newtonian fluids [5] before. The present study for the first time provides the transient response of viscoelastic fluids in 2-D film casting system.

In Fig. 7(a), the transient response of the edge film thickness for the viscoelastic cases at take-up is displayed for various draw ratios. In the stable region, initially imposed disturbance decays with time. If the draw ratio is beyond the critical value, the transient curves gradually grow and finally evolve into self-sustained periodic oscillations, i.e., limit cycles. These limit cycles at higher draw ratio become highly skewed or non-sinusoidal. Not only film thickness at the edge but also other state variables also fluctuate periodically with the same period of oscillation (Fig. 7(b)). It is seen here that when the dimensionless film thickness at the center goes through the maximum value, that at the edge becomes the minimum.

For the typical process conditions ($A_r = 0.6$ and $D_r = 32$), the transient responses of UCM fluids with different Deborah numbers were portrayed along with its Newtonian counterpart in Fig. 8. The periodic oscillations of film width at the take-up decay with time and finally disappear as Deborah number

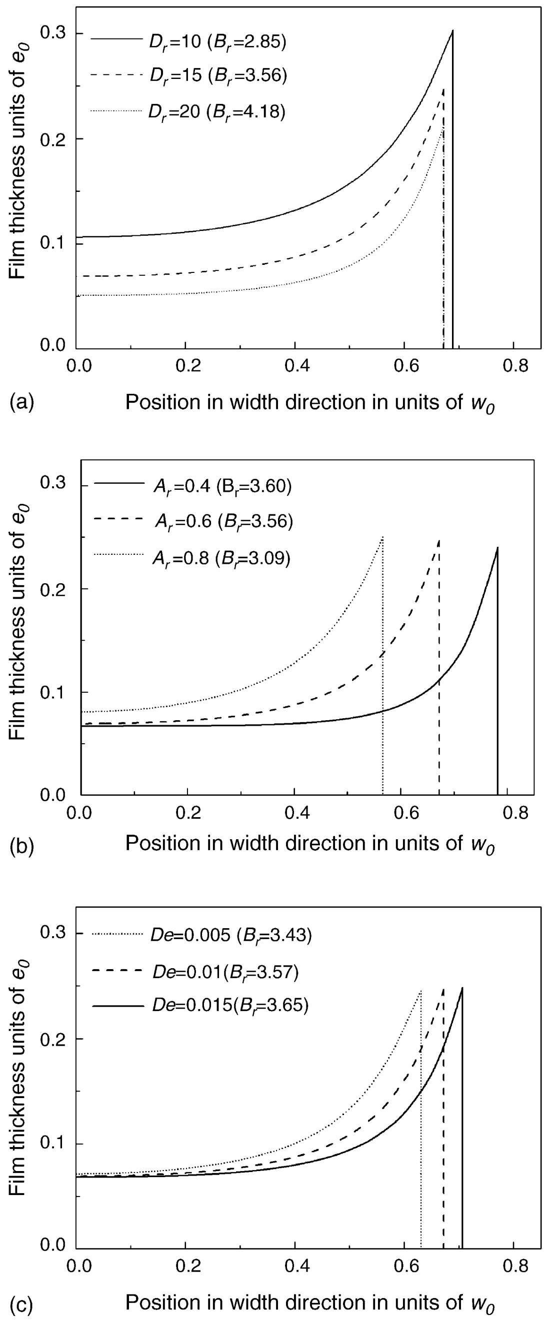

Fig. 6. Effects of various process conditions on the steady-state film thickness and edge beads with $D_r = 15$, $A_r = 0.6$, and $De = 0.01$: (a) effect of draw ratio; (b) effect of aspect ratio; and (c) effect of Deborah number.

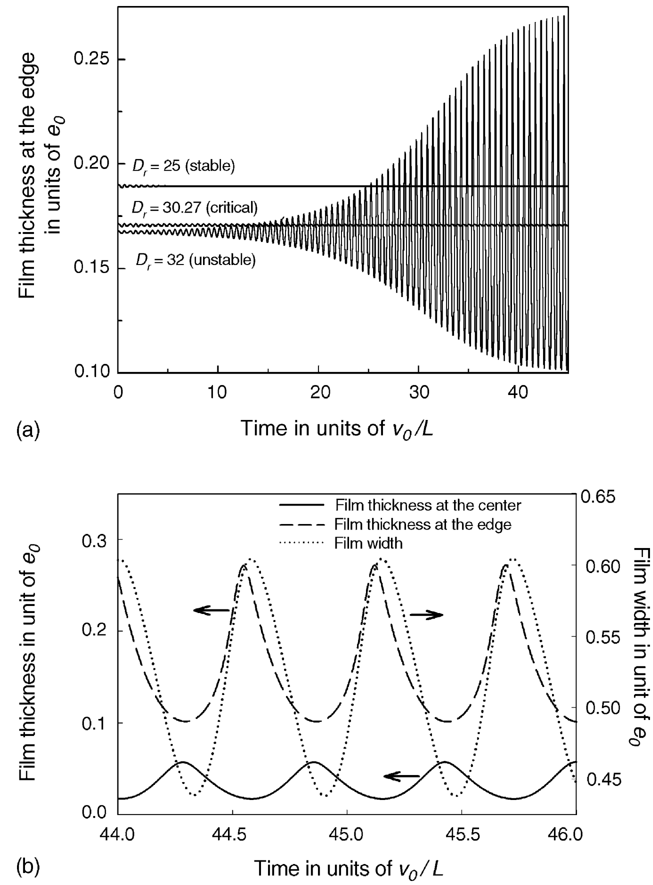

Fig. 7. Transient responses for viscoelastic fluids by the 2-D model: (a) film thickness at the edge of take-up with draw ratio ($A_r = 0.6$ and $De = 0.0017$) and (b) periodic oscillations of the film thickness and the film width at take-up at $D_r = 32$.

increases. From these results, the stabilizing effect of fluid viscoelasticity is apparent in film casting of extension thickening fluids (the fluids that normally display increasing extensional viscosity when extension rate increases with a typical example being low-density polyethylene (LDPE), whereas extension thinning fluids display decreasing extensional viscosity when extension rate increases with a typical example being high-density polyethylene (HDPE)), as already demonstrated by the previous 1-D model [6]. This stabilizing effect can also be explained by considering the tension acting on the film and the tension sensitivity, as already demonstrated in other extensional deformation processes [6,7,13]. In other words, higher tension and thus lower tension sensitivity is bestowed upon the film by higher viscoelasticity in the film casting of extension thickening fluids. This makes the system more stable and less sensitive to disturbances. Not only the fluid viscoelasticity, but also the effects of other process conditions such as aspect ratio on the

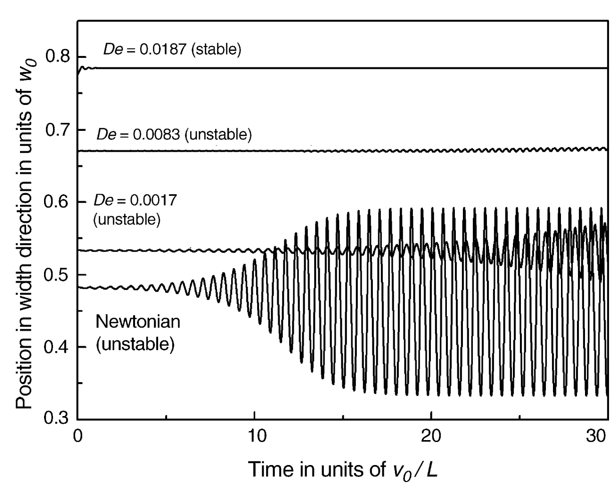

Fig. 8. Effect of fluid viscoelasticity or Deborah number on the process stability at $A_r = 0.6$ and $D_r = 32$: transient responses of film width at take-up.

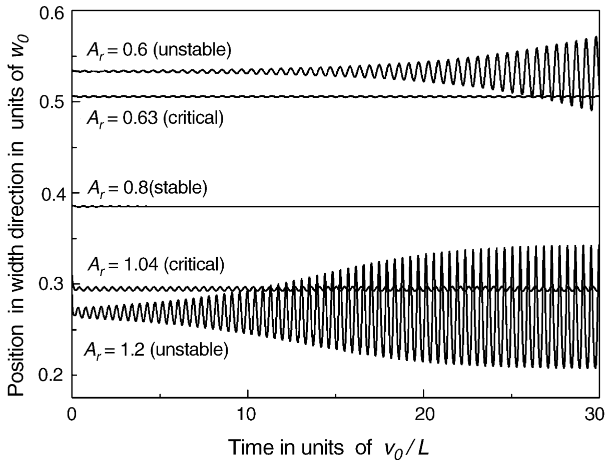

Fig. 9. Effect of aspect ratio on the process stability at $D_r = 32$ and $De = 0.0017$: transient responses of film width at take-up.

stability of viscoelastic system can also be investigated as shown in Fig. 9. The stable region interestingly exists within the intermediate aspect ratio range of 0.63 and 1.04 under the conditions of Fig. 9, exhibiting lower optimal aspect ratio in 2-D case than that (i.e., 1.5) in 1-D case as shown in Lee et al. [6].

It also has been found that the same draw resonance criterion based on the kinematic waves traveling from the die exit to the take-up, developed earlier for fiber spinning process [27], equally holds in this film casting process. Finally, it should be noted that the proposed numerical method is not restricted to the UCM model adopted for the simulations in this study for the purpose of validating the numerical formulation. It should also be applicable to other realistic constitutive equations for extensional deformation processes such as the Phan-Thien–Tanner model [29], whose results will be reported later [26].

5. Conclusion

The nonlinear transient dynamics and stability of two-dimensional (2-D) isothermal film casting process, especially focusing on the specific defects and instabilities occurring in the process, i.e., neck-in, edge beads, and draw resonance, have been investigated using newly devised numerical simulation techniques with finite element methods (FEM), capable of handling both Newtonian and viscoelastic fluids. To effectively solve the time-dependent free surface problem of this system, the Arbitrary Lagrangian Eulerian method in conjunction with a spine method was implemented as a free surface tracking method. Transient solutions of the 2-D film casting dynamics thus have been obtained through the simulation of the process for viscoelastic fluids, successfully portraying the basic flow behavior of the process as well as the three instability modes of draw resonance, neck-in and edge beads.

Acknowledgements

This study was supported by research grants from the Korea Science and Engineering Foundation (KOSEF) through the Applied Rheology Center (ARC), an official KOSEF-created engineering research center (ERC) at Korea University, Seoul, Korea.

References

[1] J.R.A. Pearson, M.A. Matovich, Spinning a molten threadline: stability, Ind. Eng. Chem. Fundam. 8 (1969) 605–609.
[2] R.J. Fisher, M.M. Denn, A theory of isothermal melt spinning and draw resonance, AIChE J. 22 (1976) 236–246.
[3] J.J. Cain, M.M. Denn, Multiplicities and instabilities in film blowing, Polym. Eng. Sci. 28 (1988) 1527–1541.
[4] N.R. Anturkar, A. Co, Draw resonance in film casting of viscoelastic fluids: a linear stability analysis, J. Non-Newtonian Fluid Mech. 28 (1988) 287–307.
[5] D. Silagy, Y. Demay, J.-F. Agassant, Stationary and stability analysis of the film casting process, J. Non-Newtonian Fluid Mech. 79 (1998) 563–583.
[6] J.S. Lee, H.W. Jung, J.C. Hyun, Frequency response of film casting process, Korea-Aust. Rheol. J. 15 (2003) 91–96.
[7] H.W. Jung, J.S. Lee, J.C. Hyun, The sensitivity and stability of spinning process using frequency response method, Korean, J. Chem. Eng. 21 (2004) 20–26.
[8] J.C. Hyun, H. Kim, J.S. Lee, H.-S. Song, H.W. Jung, Transient solutions of the dynamics in film blowing processes, J. Non-Newtonian Fluid Mech. 121 (2004) 157–162.
[9] V.R. Iyengar, A. Co, Film casting of a modified Giesekus fluid: stability analysis, Chem. Eng. Sci. 51 (1996) 1417–1430.
[10] D. Silagy, Y. Demay, J.-F. Agassant, Study of the stability of the film casting process, Polym. Eng. Sci. 36 (1996) 2614–2625.
[11] M. Beaulne, E. Mitsoulis, Numerical simulation of the film casting process, Intern. Polym. Proc. 14 (1999) 261–275.
[12] D. Acierno, L. Di Maio, C.C. Ammirati, Film casting of polyethylene terephthalate: experiment and model comparisons, Polym. Eng. Sci. 40 (2000) 108–117.
[13] J.S. Lee, H.W. Jung, H.-S. Song, K.-Y. Lee, J.C. Hyun, Kinematic waves and draw resonance in film casting process, J. Non-Newtonian Fluid Mech. 101 (2001) 43–54.
[14] K. Sakaki, R. Katsumoto, T. Kajiwara, K. Funatsu, Three-dimensional flow simulation of a film-casting process, Polym. Eng. Sci. 36 (1996) 1821–1831.
[15] S. Smith, D. Stolle, Nonisothermal two-dimensional film casting of a viscous polymer, Polym. Eng. Sci. 40 (2000) 1870–1877.
[16] N. Satoh, H. Tomiyama, T. Kajiwara, Viscoelastic simulation of film casting process for a polymer melt, Polym. Eng. Sci. 41 (2001) 1564–1579.
[17] J.M. Floryan, H. Rasmussen, Numerical methods for viscous flows with moving boundaries, Appl. Mech. Rev. 42 (1989) 323–341.
[18] C.W. Hirt, A.A. Amsden, J.L. Cook, An arbitrary Lagrangian Eulerian computing method for all flow speeds, J. Comput. Phys. 135 (1997) 203–216 (Originally published in J. Comput. Phys., 1974).
[19] J.M. Kim, K.H. Ahn, S.J. Lee, S.J. Lee, Numerical simulation of moving free surface problems in polymer processing using volume-of-fluid method, Polym. Eng. Sci. 41 (2001) 858–866.
[20] S.J. Kim, S.D. Kim, Y. Kwon, Deformation of multiple non-Newtonian drops in the entrance region, Korea-Aust, Rheol. J. 15 (2003) 75–82.
[21] A.N. Brooks, T.J.R. Hughes, Streamline upwind/Petrov-Galerkin formulations for convection dominated flows with particular emphasis on the incompressible Navier-Stokes equations, Comput. Methods Appl. Mech. Eng. 32 (1982) 199–259.
[22] K.B. Sunwoo, S.J. Park, S.J. Lee, K.H. Ahn, S.J. Lee, Numerical simulation of three-dimensional viscoelastic flow using the open boundary condition method in coextrusion process, J. Non-Newtonian Fluid Mech. 99 (2001) 125–144.
[23] B.M. Irons, A frontal solution program for finite element analysis, Int. J. Numer. Meth. Eng. 2 (1970) 5–32.

[24] S.F. Kistler, L.E. Scriven, Coating flow theory by finite element and asymptotic analysis of the Navier-Stokes system, Int. J. Numer. Meth. Fluids 4 (1984) 207–229.
[25] R. Keunings, An algorithm for the simulation of transient viscoelastic flows with free surfaces, J. Comput. Phys. 62 (1986) 199–220.
[26] J.S. Lee, D.M. Shin, J.M. Kim, H.W. Jung, J.C. Hyun, Kinematic waves and stability of two-dimensional film casting process, in preparation.
[27] H.W. Jung, H.-S. Song, J.C. Hyun, Draw resonance and kinematic waves in viscoelastic isothermal spinning, AIChE J. 46 (2000) 2106–2111.
[28] T. Dobroth, L. Erwin, Causes of edge beads in cast films, Polym. Eng. Sci. 26 (1986) 462–467.
[29] N. Phan-Thien, A nonlinear network viscoelastic model, J. Rheol. 22 (1978) 259–283.